IEEE Access
Multidisciplinary ⋮ Rapid Review ⋮ Open Access Journal

Received March 16, 2019, accepted April 7, 2019, date of publication April 16, 2019, date of current version May 13, 2019.

*Digital Object Identifier 10.1109/ACCESS.2019.2911616*

# A Simple and Accurate Method for Extracting Super Wideband Electrical Properties of the Printed Circuit Board

**YI-WEN WU[1], (Student Member, IEEE), ZHANG-CHENG HAO[1,2], (Senior Member, IEEE), MING-CUI TAO[1], XIANG WANG[1], (Student Member, IEEE), AND JIA-SHENG HONG[3], (Fellow, IEEE)**

[1]State Key Laboratory of Millimeter-Wave, School of Information Science and Engineering, Southeast University, Nanjing 210096, China
[2]Purple Mountain Laboratories, Nanjing 211111, China
[3]School of Engineering and Physical Sciences, Heriot-Watt University, Edinburgh EH14 4AS, U.K.

Corresponding author: Zhang-Cheng Hao (zchao@seu.edu.cn)

This work was supported in part by the National Natural Science Foundation of China under Grant 61471118 and Grant 61501114.

**ABSTRACT** In order to accurately design microwave, millimeter-wave components and circuits, a simple and accurate method for extracting extremely wideband characteristics of the printed circuit board (PCB), including relative dielectric constant, dielectric loss tangent, and equivalent copper conductivity, is proposed and validated in this paper. By properly selecting wideband distribution of multiple $\mathrm{TM}_{mn0}$ modes in the designed circular substrate integrated waveguide (CSIW) cavities, extremely broadband properties of PCB can theoretically be extracted with only one pair of CSIW cavities. The proposed method overcomes the limitations of conventional methods that only support narrowband applications, require a large number of cavities, and have relatively large errors. The experiments show that the proposed method is able to extract, accurately and efficiently, 8–110 GHz characteristics of a TLY-5Z substrate-based PCB and the extracted results are verified by designing and measuring the fourth-order Chebyshev filter at *X*-band.

**INDEX TERMS** Dielectric constant, dielectric loss tangent, equivalent conductivity, circular substrate integrated waveguide (CSIW) cavity, wideband characteristics.

## I. INTRODUCTION

The investigation of microwave, millimeter-wave or terahertz components and circuits based on various technologies such as the printed-circuit-board (PCB) technology [1]–[7] and the low-temperature co-fired ceramic (LTCC) technology [8]–[14] has drawn tremendous attentions due to rapid development of modern wireless systems recently. The dielectric and metal characteristics play an important role in the design of microwave and millimeter-wave components, especially at high millimeter-wave frequency. However, these characteristics provided by PCB manufactures are usually only accurate for narrowband and low frequency applications. To this end, many efforts have been made to measure those characteristics for the accurate design of millimeter-wave or terahertz components, including the transmission/reflection method [15], [16] and the resonator method [17]–[22]. The substrate integrated waveguide (SIW) technology has come into notice in recent years because of the merits of easy integration, high unloaded quality factor (Q-factor) and low cost [23]–[29]. In addition, the leakage loss is negligible with suitable spacing and size of metallized via-holes. Hence, it has been adopted to extract the characteristics of PCB [17]–[21]. Generally, the transmission/reflection method can be used to extract the wideband electrical characteristics of PCB with a relatively low accuracy. Compared to the transmission/reflection method, the resonator method has a higher accuracy [18]. However, the traditional resonator methods based on rectangular substrate integrated waveguide (RSIW) resonators suffer from single frequency or narrowband applications. For example, the frequency bandwidth must meet the limitation that: $f_H/f_L < 2.12$ [18]–[21]. To extract wideband material characteristics, a large number of cavities, which are designed to resonant at different frequencies, have to be used in the experiment. Hence, it not only needs a complex design for a large number

The associate editor coordinating the review of this manuscript and approving it for publication was Wenjie Feng.

of cavities, but also requires tedious measurements for each cavity, which leads to an increased measurement error as well, especially for millimeter-wave or terahertz application. For example, tens or dozens of cavities have to be adopted in the experiment in order to obtain the 8-60 GHz characteristics of PCB [19], [20].

For accurate design of microwave, millimeter-wave components and circuits, a simple and accurate method based on the resonator method is proposed for extracting extremely wideband characteristics of PCB by using CSIW cavities in this paper. The principle for extracting equivalent metal conductivity, dielectric loss tangent and relative dielectric constant is discussed in detail in the Section II. In Section III, the proposed method is demonstrated by experiments for extracting the 8-110 GHz characteristics of a Taconic TLY-5Z based PCB with high efficiency and accuracy, and detailed discussions are presented in the Section IV. Then, the results are verified by a fourth-order Chebyshev filter at X band in Section V. Finally, the conclusion is summarized in the Section VI.

## II. EXTRACTING PRINCIPLE

It is well known that in order to extract the electrical characteristics of a material by using the resonator method with a high accuracy, the Q-factor of the employed resonator is expected to be as high as possible. In theory, various types of PCB resonators could be used for the PCB material characteristics extraction, including the microstrip resonator, the coplanar waveguide resonator, the stripline resonator as well as the SIW resonator [17]–[22]. Compared with the other types of PCB resonators, the SIW resonator may be the best choice because it can provide much high quality factors even at W-band or above [7]. In addition, among various types of SIW resonators, the CSIW cavity, which has a higher Q-factor, better fabrication tolerance and a more compact size than the other types of SIW resonators [30], is more attractive for the high frequency material characteristics extraction. In addition, CSIW cavity has a more broadband frequency bandwidth compared with RSIW resonators, because the appearance of resonating modes in CSIW resonator follows the rule of the root of Bessel function shown in Fig. 2 which ensures a good selection of resonating modes for broadband and accurate characteristics extraction of PCB. Therefore, the CSIW resonators with weak excitations shown in Fig.1 with different substrate thicknesses are deployed in the proposed method. Different to the traditional resonator method which only utilizes one resonating mode to extract electrical characteristics [19], numerous resonating modes of the CSIW cavity are deployed in the proposed method. Since all resonating modes, excluding the degenerate mode, resonate at different frequencies and are distributed within an unlimited frequency band, the higher order modes are exploited to extract wider frequency band electrical characteristics of PCB [31].

As shown in Fig.1, grounded coplanar waveguide (GCPW) provides weak excitations for CSIW resonators due to the good dispersion characteristics in millimeter-wave bands. And the transmission loss from GCPW to the CSIW resonator hardly affects the Q-factor of CSIW resonator because of the weak excitations. Supposing the substrate thickness is less than one half-wavelength, the CSIW resonator only supports $TM_{m,n,0}$ resonating modes because the Ø direction component of the $TE_{m,n,k}$-mode electrical field cannot be supported due to the discontinuity of metallic vias which form the sidewall of the circular SIW resonator. Then, the resonant frequency can be expressed as [32]:

$$f_{TM_{m,n,0}} = \frac{C_0}{\sqrt{\varepsilon_r}} \frac{\nu_{m,n}}{2\pi R_{eff}} \tag{1}$$

where $C_0$ is the speed of light in vacuum, $R_{eff}$ is the effective radius of the CSIW resonator, $\nu_{m,n}$ is the *nth* root of the Bessel function of order $m$, and $\varepsilon_r$ is the equivalent relative permittivity of the substrate.

From (1), it can be seen that once the effective radius, $R_{eff}$, of the CSIW resonator is determined, the operating frequency can be calculated by properly choosing the operating mode. Two CSIW resonators with different thicknesses are deployed in the proposed method. These two resonators have the same $TM_{m,n,0}(m = 0..M_0, n = 1..N_0)$ resonating modes. By measuring the loaded Q-factor of all those modes, their unloaded Q-factor can be deduced. Then the electrical characteristics of PCB can be extracted by individually comparing the unloaded

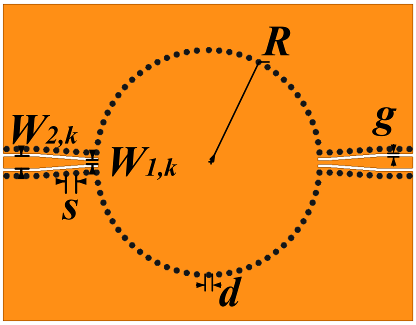

**FIGURE 1.** Layout of the adopted CSIW cavity for extracting wideband PCB material characteristics.

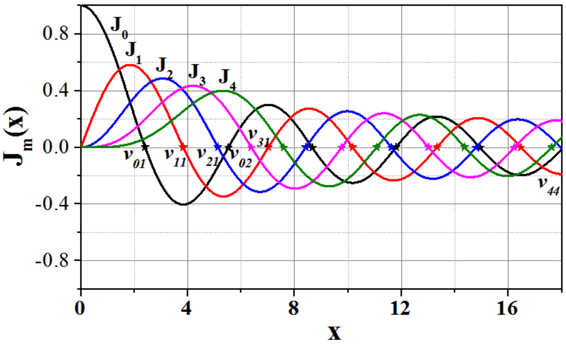

**FIGURE 2.** High order Bessel function curves. Note: 1. $J_m(x) = \sum_{k=0}^{\infty} \frac{(-1)^k}{k!\Gamma(k+m+1)}(\frac{x}{2})^{2k+m}$, the Bessel function of order m. 2. $v_{mn}$ is the nth root of the Bessel function of order m.

Q-factors of each pair of corresponding resonating modes of the two CSIW resonators. Consequently, the operating frequency bandwidth covers from the resonating frequency of the fundamental mode to that of the highest selected mode. It should be mentioned that the proposed method is especially suitable for high millimeter-wave frequency extraction due to the high-order resonating mode has a much higher Q-factor than that of the fundamental resonating mode. The detailed extracting process is explained in the following sections.

### A. DETERMINING THE RADIUS OF THE CSIW RESONATOR

The radius of the CSIW resonator is related to the radius of a circular waveguide resonator, i.e. $R_{eff}$. As can be seen from (1), once the lowest operating frequency $f_L$ of the material characteristics under extraction is preassigned and the initial relative dielectric constant is given by the manufacture, the equivalent radius $R_{eff}$ of the CSIW resonator can be initially obtained from the relationship of the resonating frequency of the fundamental mode, i.e., the $TM_{0,1,0}$ mode, and $R_{eff}$, as (2) [32]. Then the frequency interval $(\Delta f_{m1,n1;m2,n2})$ between two adjacent modes ($TM_{m1,n1}$ and $TM_{m2,n2}$) of the material characteristics under extraction is calculated according to (3). Generally, a higher mode at the lowest frequency leads to a narrower bandwidth and a smaller frequency interval. Because some neighboring high-order modes are too close to each other in higher frequency band, which is difficult to distinguish between them. In order to extract broadband characteristics of PCB, the fundamental mode is selected as the first mode.

$$R_{eff} = \frac{C_0}{\sqrt{\varepsilon_r}} \frac{\nu_{m,n}(or\ \nu_{0,1})}{2\pi f_L(or\ f_{TM_{0,1,0}})}; \quad \nu_{0,1} = 2.405 \tag{2}$$

$$\Delta f_{m1,n1;m2,n2} = \frac{C_0}{\sqrt{\varepsilon_r}} \frac{\nu_{m2,n2} - \nu_{m1,n1}}{2\pi R_{eff}} \tag{3}$$

$$\frac{h}{R_{eff}} \leq 2.1 \tag{4}$$

$$2R_{eff} = 2\mathrm{R} - \frac{d^2}{0.95s} \tag{5}$$

where $C_0$ is the speed of light in vacuum, $R_{eff}$ is the effective radius of the CSIW resonator, $R$ is the physical radius of the CSIW resonator, $d$ is the radius of the metallized via-hole, and $s$ is the spacing between the metallized via-holes.

In addition, to support the fundamental mode, the $TM_{0,1,0}$ mode, the thickness of the substrate should satisfy (4) [32], and then an empirical relationship in (5) between the physical radius and the equivalent radius of the CSIW resonator can be obtained by the guidelines of RSIW [7].

### B. UNLOADED Q-FACTOR OF THE CSIW RESONATOR

Theoretically, all the resonating modes of the CSIW resonator can be adopted for the material characteristics extraction. However, considering the planar excitation topology and easy measurement, only $TM_{m,n,0}$-mode is deployed in the extraction. The electromagnetic field of $TM_{m,n,0}$-mode in a CSIW resonator can be expressed as [33]:

$$\begin{aligned} E_\rho &= E_\varphi = H_z = 0 \\ E_z &= 2k_c^2 D J_m(k_c\rho)\cos(m\varphi) \\ H_\rho &= -j\frac{2\omega\varepsilon m}{\rho} D J_m \sin(m\varphi) \\ H_\varphi &= -j2\omega\varepsilon k_c J_m^{'}(k_c\rho)\cos(m\varphi) \\ k_c &= \frac{\nu_{m,n}}{R} \end{aligned} \tag{6}$$

where m $= 0, 1, 2\cdots$ ; n $= 1, 2, 3\cdots$.

The unloaded Q-factor ($Q_{u_{m,n}}$) of the $TM_{m,n,0}$-mode can be expressed as [18]:

$$\frac{1}{Q_{u_{m,n}}} = \frac{1}{Q_{D_{m,n}}} + \frac{1}{Q_{c1_{m,n}}} + \frac{1}{Q_{c2_{m,n}}} \tag{7}$$

where $Q_{c1_{m,n}}$ is resulting from the conductor loss of the metallic-via sidewall of the CSIW resonator, $Q_{c2_{m,n}}$ represents the conductor loss from top and bottom surfaces of the CSIW resonator, and $Q_{D_{m,n}}$ is associated with the loss from the dielectric material, which can be represented as tan$\delta$ of the dielectric material.

In the measurement, weak coupling circuits shown in Fig. 1 can be used to extract the unloaded Q-factor $Q_{u_{m,n}}$ from the loaded Q-factor $Q_{L_{m,n}}$ and the coupling coefficients of the input/output ports as following [21]:

$$\begin{aligned} Q_{u_{m,n}} &= Q_{L_{m,n}}\left(1 + \beta_{1_{m,n}} + \beta_{2_{m,n}}\right) \\ Q_{L_{m,n}} &= \frac{f_{TM_{m,n,0}}}{\Delta f_{m,n,0}} \\ 2\beta_{1_{m,n}} &= \frac{S_{21,m,n}}{1 - S_{21,m,n}} \quad i = 1, 2. \end{aligned} \tag{8}$$

where $Q_{L_{mn}}$ is the loaded Q-factor for the $TM_{m,n,0}$ mode, $S_{21,m,n}$ is the magnitude of the transmission coefficient at resonant frequency, $f_{TM_{m,n,0}}$ is the resonating frequency of the $TM_{m,n,0}$-mode, and $\Delta f_{m,n,0}$ is the 3-dB bandwidth of the transmission coefficient. $\beta_{1mn}$ and $\beta_{2m,n}$ are the coupling coefficients, which are almost equal due to the symmetrical structures in Fig.1 when the loss of material is not so serious. Then, the $Q_{u_{m,n}}$ can be extracted by (9)

$$Q_{u_{m,n}} = \frac{f_{TM_{m,n,0}}}{\Delta f_{m,n,0}} \frac{1}{1 - S_{21,m,n}} \tag{9}$$

The conductive loss includes the loss from the metallic-via sidewall, and top and bottom surfaces of the CSIW resonator. It can be expressed by using the conductive quality factor Q-factor, i.e. $Q_c$ as:

$$\frac{1}{Q_{c_{m,n}}} = \frac{1}{Q_{c1_{m,n}}} + \frac{1}{Q_{c2_{m,n}}} \tag{10}$$

The $\mathrm{Q_{c_{m,n}}}$, $Q_{c1_{m,n}}$ and $Q_{c2_{m,n}}$ can be calculated using the definition of Q-factor:

$$\begin{aligned} Q_c &= \omega\frac{W}{P_{L1} + P_{L2}} \\ W &= (W_e)_{max} = \frac{h\varepsilon}{2}\int_0^{R_{eff}}\int_0^{2\pi} |E_z|^2 \rho\, d\rho\, d\varphi \end{aligned}$$

$$P_{L1} = \frac{1}{2}R_s h \int_0^{2\pi} |H_\varphi|^2_{\rho=R_{eff}} + |H_\rho|^2_{\rho=R_{eff}}\, d\varphi$$
$$P_{L2} = \frac{1}{2}R_s \int_0^{R_{eff}} \int_0^{2\pi} |H_\varphi|^2 + |H_\rho|^2 d\rho d\varphi \qquad (11)$$

And, it can be expressed as

$$\frac{1}{Q_{c_{m,n}}} = \frac{1}{Q_{c1_{m,n}}} + \frac{1}{Q_{c2_{m,n}}} = \sqrt{\frac{\varepsilon}{\mu}}\frac{2R_s k}{v_{m,n}} + \sqrt{\frac{\varepsilon}{\mu}}\frac{2R_s}{v_{m,n}}\frac{R_{eff}}{h}$$
$$\mathrm{k} = \frac{dN}{2R_{eff}} q_1 \qquad (12)$$

where $N$ is the number of metallic vias of the CSIW sidewall, $d$ is the diameter of the metallic-via, $R_{eff}$ is the effective radius of the CSIW resonator and $R_s$ is the resistivity of metal surface. Since the currents of the resonating electromagnetic fields are non-uniformly distributed along the surface of each metallic-via, i.e. the inner surface has much stronger currents than that of the outer surface, an empirical coefficient of $q_1 = 0.53$ is used to represent the surface utilization ratio of metallic vias in the sidewall.

Based on above discussions, the unloaded Q-factor ($Q_{um,n}$) of the $TM_{m,n,0}$-mode in a CSIW resonator can be explicitly expressed as:

$$Q_{u_{m,n}} = tan\delta + \sqrt{\frac{\varepsilon}{\mu}}\frac{2R_s k}{v_{m,n}} + \sqrt{\frac{\varepsilon}{\mu}}\frac{2R_s}{v_{m,n}}\frac{R_{eff}}{h} \qquad (13)$$

### C. EFFECTIVE CONDUCTIVITY OF THE METAL

Two CSIW cavities with different heights, i.e., $h_1$ and $h_2$, have been used to extract the characteristics of PCB. Supposing the two unloaded Q-factor, i.e., $Q_{u1m,n}$ and $Q_{u2m,n}$, are measured with the circuit model shown in Fig.1, the conductor loss can be obtained by subtracting (13) with different thicknesses, and then

$$R_s = \frac{v_{m,n}}{2R_{eff}}\sqrt{\frac{\mu}{\varepsilon}}\frac{Q_{u2_{m,n}} - Q_{u1_{m,n}}}{Q_{u2_{m,n}}Q_{u1_{m,n}}}\frac{h_2 - h_1}{h_2 h_1} \qquad (14)$$

where $\varepsilon$ is the equivalent dielectric permittivity which can be extracted from the resonating frequency of the $TM_{m,n,0}$-mode, as shown in the next part, and $\mu = \mu_0 = 4\pi \times 10^{-7} H/m$ for a non-magnetic material. Considering the relationship between effective conductivity and equivalent resistivity of metal surfaces in (15), the equivalent conductivity can be extracted and expressed as (16):

$$R_s = \sqrt{\frac{\omega_{mn}\mu}{2\sigma}}, \quad \omega_{mn} = \frac{2\pi}{\lambda_{mn}\sqrt{\mu\varepsilon}}, \quad \lambda_{mn} = \frac{2\pi R_{eff}}{v_{mn}} \qquad (15)$$
$$\sigma_{eff} = \frac{4\pi f_{TM_{mn0}} R_{eff}^2}{v_{mn}^2}\varepsilon\left(\frac{Q_{u2}Q_{u1}}{Q_{u2} - Q_{u1}}\right)^2\left(\frac{h_2 - h_1}{h_2 h_1}\right)^2 \qquad (16)$$

### D. EXTRACTING THE COMPLEX PERMITTIVITY OF THE DIELECTRIC SUBSTRATE

If the effective conductivity is obtained as discussed in the part C, the equivalent dielectric loss tangent can be deduced by substituting the resistivity of metal surface, $R_s$, into (13), and can be expressed as:

$$\tan\delta = \frac{1}{h_2 - h_1}\left[\frac{h_2}{Q_{u2}}\left(k + \frac{h_2}{R_{eff}}\right) - \frac{h_1}{Q_{u1}}\left(k + \frac{h_1}{R_{eff}}\right)\right] \qquad (17)$$

On the other hand, with the measurement of resonant frequencies of the $TM_{mn0}$ mode, the equivalent relative dielectric constant at resonating frequency can be obtained and expressed as (18):

$$\varepsilon_r = \frac{C_0^2 v_{mn}^2}{f_{TM_{mn0}}^2 4\pi^2 R_{eff}^2} \qquad (18)$$

## III. EXPERIMENTAL RESULTS

In this section, the proposed method has been used to extract the 8-110 GHz equivalent dielectric characteristics and conductivity for PCB. As a typical substrate for the design of microwave and millimeter-wave components, the Taconic TLY-5Z substrate is adopted in the commercial PCB fabrication process. According to the manufacture [34], the substrate has a relative dielectric constant of 2.2 ± 0.04 and a loss tangent of 0.001 at 1.9 GHz. The 0.035 mm thick copper is used as metal material in the PCB process for the fabrication of the circuits. Considering the measuring limitation, we divide the 8-110 GHz frequency band into three parts, i.e. 8-60 GHz, 60-75 GHz and 75-110 GHz, and extract the equivalent dielectric characteristics and conductivity for those three frequency bands individually. For 8-60 GHz frequency band, a pair of CSIW resonators with 0.254 mm and 0.508 mm thickness have been measured by using the Anritsu Test Fixture SC5225 [35], and the conventional waveguide interface is used to measure the responses of a pair of CSIW resonators for the other two frequency bands, respectively. This is because that the highest operating frequency of the Anritsu Test Fixture SC5225 is 60 GHz. The detailed extraction process will be discussed in the following parts.

### A. EXTRACTION OF THE ELECTRICAL PROPERTIES OF THE TLY-5Z PCB WITHIN 8-60 GHZ

To extract the 8-60 GHz equivalent dielectric characteristics and conductivity, the resonating frequency of the fundamental mode, i.e. $TM_{0,1,0}$ mode, in the CSIW resonator is chosen as 7.9 GHz. Hence, the radius of the circular resonator can be obtained from (2) as $R_{eff} = 9.78mm$. In order to improve the accuracy of the extraction results, the adjacent frequency interval $\left(\frac{(f_n - f_{n-1})}{0.5(f_n + f_{n-1})} * 100\%\right)$ among the selected modes exceeds 15%. The highest mode is chosen as the $TM_{4,4,0}$ mode whose resonating frequency is 58.431 GHz. Two planar circuits shown in Fig. 1 are designed for the extraction process. All the geometries of the two designed CSIW resonators are the same, except their thicknesses, which are 0.254 mm and 0.508 mm, respectively. The dimensions of the designed circuits are shown in Table 1, and two fabricated prototypes are shown in Fig. 3. An Anritsu test fixture SC5225 and a Keysight VNA have been used to measure the $S_{21}$ responses

**TABLE 1.** Dimensions of the CSIW resonators (Unit: mm).

| $W_{1,1}$ | $W_{2,1}$ | $W_{1,2}$ | $W_{2,2}$ | $s$ | $d$ | $R$ | $Gap$ |
|---|---|---|---|---|---|---|---|
| 0.45 | 0.58 | 0.5 | 0.97 | 0.5 | 0.3 | 9.87 | 0.15 |

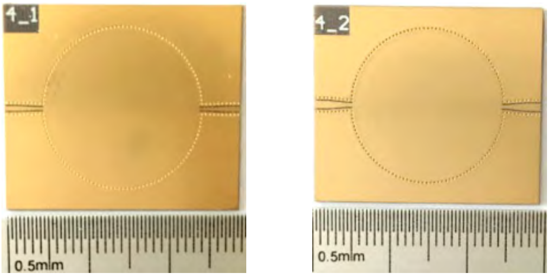

(a) (b)

**FIGURE 3.** Photographs of the fabricated prototypes for the 8-60 GHz extraction. (a) $h_1 = 0.254$ mm; (b) $h_2 = 0.508$ mm.

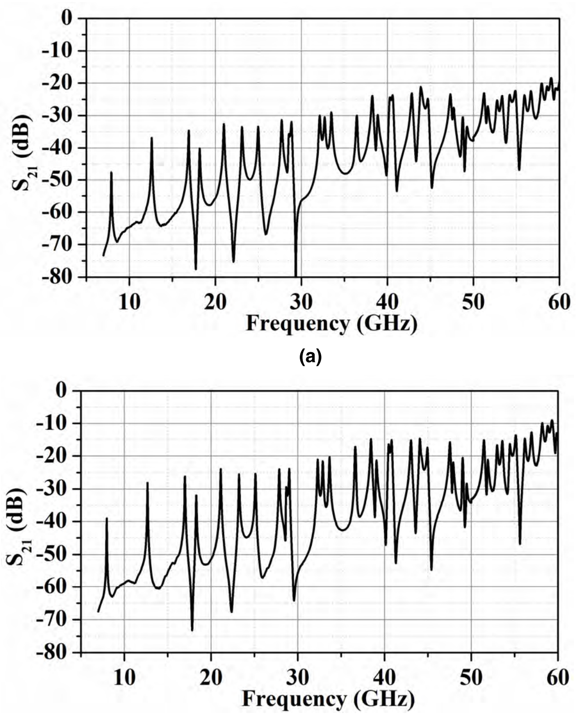

(b)

**FIGURE 4.** Measured transmission coefficients of CSIW cavities. (a) $h_1 = 0.254$ mm; (b) $h_2 = 0.508$ mm.

of those two circuits, which are shown in Fig.4 (a) and (b), respectively.

As shown in Fig. 4, the two measured transmission coefficients have almost the same resonant pattern due to the same radius of CSIW resonator. However, their magnitudes differ by at least 10 dB. Thicker resonator has a higher unloaded Q-factor than that of thinner resonator at the same resonating frequency, which leads to a higher magnitude of $S_{21}$ even with a weak excitation shown in Fig. 4(b). It should be noticed that a larger $S_{21}$ is obtained at higher frequency. This is resulted by the high-order resonating mode which has a much high quality factor than that of the fundamental mode. This would be very useful for high frequency measurement because measured $S_{21}$ may be too low to be accepted if a fundamental mode is adopted in the extracting process.

Table 2 compares the extracted resonating frequencies of different resonating modes from the full-wave simulated and measured results. In the simulation, the relative dielectric constant always keeps unchanged as 2.2, while it may be varied along with operating frequency in the experiment. Hence, the simulation can be used as a reference for the experimental extraction. In addition, it can be noticed that there exists a small discrepancy between the resonating frequencies of 0.254 mm and 0.508 mm thick CSIW cavities for both cases of simulation and measurement. This is resulting from the different quality factors of the CSIW cavities. Generally, higher quality factor leads to sharper resonating peaks and a more accurate extraction result. However, thicker substrate requires a wider 50 ohm GCPW for excitation. When the extraction bandwidth is extremely wide, a wide 50 ohm GCPW needs to be avoided to keep that only the quasi-TEM mode is propagated along the GCPW for circuit excitations.

Table 3 presents the extracted equivalent dielectric characteristics of the TLY-5Z substrate and the effective conductivity of copper in PCB process. These are illustrated in Fig. 5 together with the equivalent dielectric loss tangent of Taconic TLY-5. As expected, the effective conductivity decreases as the operating frequency increases, while the equivalent loss tangent is increased. As shown in Fig. 5. (c), the extracted dielectric constant of the PCB keeps unchanged as 2.2 within 8-60 GHz.

### B. EXTRACTION OF THE ELECTRICAL PROPERTIES OF THE TLY-5Z PCB WITHIN V-BAND AND W-BAND

As discussed above, since the conventional SMA only supports an operating frequency below 60 GHz, the dielectric characteristics and conductivity of PCB for operating frequencies beyond 60 GHz. Since the V-band extraction process is similar to that of the W-band extraction process, only W-band extraction process is discussed in detail in the rest of this part. Fig. 6 shows the circuit model for the extraction of the V- and W- bands and the corresponding geometries are presented in Table 4 and 5, respectively. The waveguide interface is adopted to extract the equivalent CSIW resonator is excited by the standard rectangular waveguide (WR10) at the input/output ports through SIW transmission lines within W band. Due to the operating frequency bandwidth limitation of the standard WR10 waveguide, the extracted frequency is limited within 75-110 GHz.

Different to the extraction process in the part A where a fundamental resonating mode is adopted for the lowest frequency, a high-order resonating mode is selected in this process for the lowest frequency around 75.0 GHz due to the fundamental mode has a poor quality factor at such high frequency. Consequently, the $TM_{430}$ mode is selected with a resonating frequency of around 78.0 GHz for the extraction

**TABLE 2.** Extracted resonant frequencies within 8-60 GHz.

| Resonant mode | $v_{mn}$ | Extracted from Simulations (GHz) | | Extracted from experiments (GHz) | |
|---|---|---|---|---|---|
| | | 0.254mm | 0.508mm | 0.254mm | 0.508mm |
| *TM010* | 2.4048 | 7.965 | 7.977 | 7.9013 | 7.9581 |
| *TM110* | 3.8317 | 12.692 | 12.702 | 12.6088 | 12.6788 |
| *TM210* | 5.1356 | 17.016 | 17.021 | 16.9138 | 16.9659 |
| *TM020* | 5.5201 | 18.316 | 18.331 | 18.1913 | 18.3006 |
| *TM310* | 6.3802 | 21.149 | 21.165 | 21.0041 | 21.1156 |
| *TM120* | 7.0155 | 23.255 | 23.265 | 23.1172 | 23.2222 |
| *TM410* | 7.5883 | 25.156 | 25.171 | 25.0006 | 25.1187 |
| *TM220* | 8.4172 | 27.909 | 27.922 | 27.7372 | 27.8619 |
| *TM320* | 9.7610 | 32.348 | 32.351 | 32.1734 | 32.3178 |
| *TM130* | 10.1735 | 33.741 | 33.757 | 33.5384 | 33.6063 |
| *TM420* | 11.0647 | 36.710 | 36.715 | 36.4113 | 36.5763 |
| *TM040* | 11.7915 | 38.538 | 38.553 | 38.2881 | 38.4531 |
| *TM330* | 13.0152 | 43.166 | 43.169 | 42.8937 | 43.0875 |
| *TM430* | 14.3725 | 47.639 | 47.657 | 47.3687 | 47.4223 |
| *TM530* | 15.7002 | 51.675 | 51.702 | 51.2263 | 51.4619 |
| *TM440* | 17.6160 | 58.424 | 58.431 | 57.9416 | 58.1772 |

**TABLE 3.** Extracted effective relative dielectric constant and equivalent conductivity within 8-60 GHz.

| Resonant mode | Effective relative dielectric constant | | Equivalent conductivity | |
|---|---|---|---|---|
| | 0.254mm | 0.508mm | 0.254mm | 0.508mm |
| *TM010* | 2.2357 | 2.2107 | 2.1858E+07 | 2.2015E+07 |
| *TM110* | 2.2293 | 2.2084 | 1.7396E+07 | 1.7492E+07 |
| *TM210* | 2.2280 | 2.2061 | 1.4862E+07 | 1.4948E+07 |
| *TM020* | 2.2306 | 2.2076 | 1.3606E+07 | 1.3688E+07 |
| *TM310* | 2.2305 | 2.2107 | 1.1889E+07 | 1.1952E+07 |
| *TM120* | 2.2273 | 2.2083 | 1.1367E+07 | 1.1424E+07 |
| *TM410* | 2.2276 | 2.2094 | 1.0528E+07 | 1.0578E+07 |
| *TM220* | 2.2275 | 2.2093 | 9.1431E+06 | 9.1863E+06 |
| *TM320* | 2.2277 | 2.2102 | 8.8113E+06 | 8.8547E+06 |
| *TM130* | 2.2267 | 2.2099 | 8.8832E+06 | 8.9287E+06 |
| *TM420* | 2.2250 | 2.2041 | 8.9790E+06 | 9.0246E+06 |
| *TM040* | 2.2271 | 2.2107 | 8.5700E+06 | 8.6154E+06 |
| *TM330* | 2.2280 | 2.2085 | 8.2767E+06 | 8.3141E+06 |
| *TM430* | 2.2301 | 2.2121 | 7.8845E+06 | 7.9231E+06 |
| *TM530* | 2.2301 | 2.2107 | 7.0929E+06 | 7.1255E+06 |
| *TM440* | 2.2300 | 2.2112 | 6.5337E+06 | 6.5656E+06 |

at the lowest frequency. Hence, the effective and physical radiuses of CSIW resonant, i.e., $R_{eff}$ and $R$, can be obtained as 5.91mm and 6mm from (2)-(5). Then, the $TM_{160}$ mode is adopted for the highest frequency extraction, which has a resonating frequency around 108.0 GHz. Similarly, two circuits with the same CSIW resonators but different thicknesses have been used for the extraction process. As explained above, thick substrates have been used for improving the quality factor of the CSIW resonator as well as improving the extraction accuracy, whose thicknesses are 0.508 mm and 1.016 mm, respectively.

**TABLE 4.** Dimensions of the CSIW resonators at W-Band (Unit: mm).

| *W_siw* | *L_siw* | *R* | *d* | *W_slot* | *L_slot* | *L_dis* |
|---|---|---|---|---|---|---|
| *2.2* | *10.4* | *6* | *0.3* | *0.4* | *0.6* | *1.4* |

**TABLE 5.** Dimensions of the CSIW resonators at V-Band (Unit: mm).

| *W_siw* | *L_siw* | *R* | *d* | *W_slot* | *L_slot* | *L_dis* |
|---|---|---|---|---|---|---|
| *2.6* | *10.4* | *8.19* | *0.3* | *0.5* | *0.8* | *1.8* |

Photographs of the fabricated two prototypes at W band are presented in Fig. 7, and the Keysight VNA is used to measure individually the $S_{21}$ responses of those two prototypes with the WR10 interfaces, as shown in Fig. 8. By using the proposed method, the extracted resonant frequencies from full-wave simulated and measured results are presented in Table 6. Because the designed resonators can provide enough high quality factors, almost same resonant frequencies can be found in Table 6 for each resonating modes in

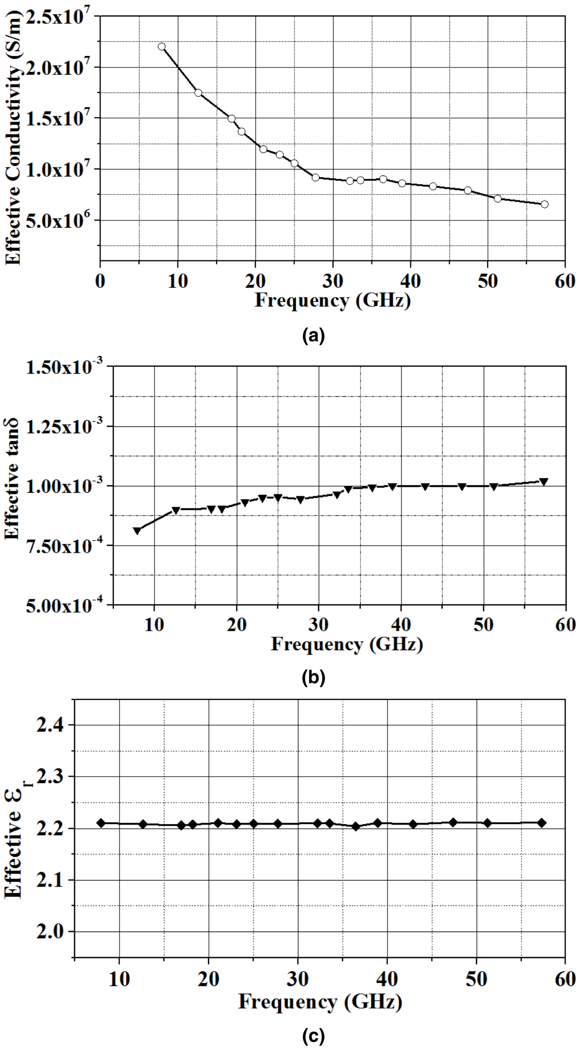

(a)

(b)

(c)

**FIGURE 5.** Extracted equivalent dielectric properties and conductivity of a TYL-5Z PCB within 8-60 GHz; (a) conductivity; (b) dielectric loss tangent; (c) relative dielectric constant from $h = 0.508$ mm thick substrate.

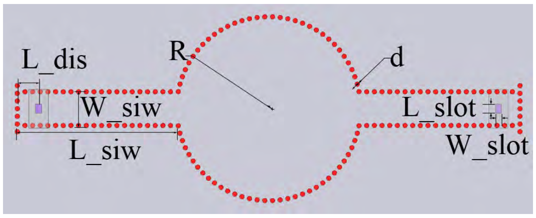

**FIGURE 6.** Layout of the circuit model for the V-band and W-band extraction.

CSIW resonators with different thicknesses. The extracted equivalent complex dielectric permittivity and effective conductivity are presented in Table 7.

Similarly, two CSIW cavities are designed for the V-band extraction, in which the $TM_{150}$ mode and $TM_{250}$ mode are selected with resonating frequencies of 65.5 GHz and 71.0 GHz for the lowest and the highest frequency, respectively. The results of extraction at V band and W band are illustrated in Fig. 9. With the increasing of the operating frequency, the dielectric substrate loss increases quickly, and the effective conductivity of the copper used in the PCB process becomes worse. However, the TLY-5Z substrate has a very stable relative dielectric constant, even at 108 GHz.

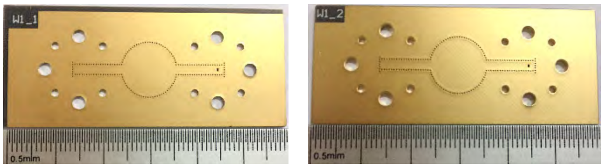

(a) (b)

**FIGURE 7.** Photographs of fabricated prototypes for the W-band.

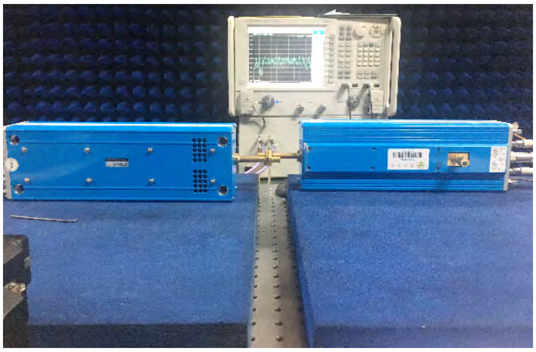

**FIGURE 8.** Measurement setup for the W-band extraction.

## IV. DISCUSSIONS

The overall extracted results from 8-110 GHz for the TLY-5Z substrate based PCB are plotted in Fig.10. It can be seen from Fig.10 (a) and (c) that the conductivity of the PCB under test drops from 8 to 110 GHz, while the dielectric loss increases monotonously as the frequency increases. In addition, the TLY-5Z substrate has a stable relative dielectric constant of 2.2 within 8-110 GHz, as illustrated in Fig.10 (c).

It should be mentioned that different substrate thicknesses and resonating modes have been adopted for the extraction of three frequency-bands mentioned above. That is based on the following criteria:

### A. THE CHOICE OF THE SUBSTRATE THICKNESS

Generally, a CSIW cavity with a thicker substrate has a higher quality factor which leads to a more accurate extraction result. On the one hand, the substrate thickness should be less than half-wavelength to avoid the appearance of $TM_{mnp}$ mode ($p \neq 0$). For example, the selected substrate thicknesses at the W-band are 0.508 mm and 1.016 mm in this paper because one half-wavelength at 100 GHz in a CSIW cavity is about 1.011 mm. In addition, the selected substrate thickness should keep the excitation port only supports single-mode excitation. For example, GCPW can not keep a good transmission from 8 to 60 GHz when the substrate thickness is 1.016mm due to a too wide 50 ohm GCPW. Therefore, the selected substrate

**TABLE 6.** Extracted resonant frequencies within W-band.

| Resonant mode | $v_{mn}$ | Extracted from Simulations (GHz) | | Extracted from Experiments (GHz) | |
|---|---|---|---|---|---|
| | | h1=0.508mm | h2=1.0168mm | h1=0.508mm | h2=1.016mm |
| *TM430* | 14.37254 | 78.119 | 78.146 | 78.0121 | 78.1286 |
| *TM530* | 15.70017 | 85.18 | 85.19 | 84.9293 | 85.1536 |
| *TM340* | 16.22347 | 89.148 | 89.211 | 88.9943 | 89.1764 |
| *TM920* | 17.24122 | 95.082 | 95.15 | 94.9529 | 95.1829 |
| *TM730* | 18.28758 | 99.374 | 99.261 | 99.27 | 99.4986 |
| *TM350* | 19.40942 | 105.01 | 105.047 | 104.8741 | 105.1534 |
| *TM160* | 19.61586 | 108.126 | 108.19 | 108.0669 | 108.2825 |

**TABLE 7.** Extracted equivalent relative dielectric constant and effective conductivity within W-band.

| Resonant mode | Equivalent relative dielectric constant | | Effective conductivity | |
|---|---|---|---|---|
| | h1=0.508mm | h2=1.016mm | h1=0.508mm | h2=1.016mm |
| *TM430* | 2.2074 | 2.2043 | 4.9220E+06 | 4.9144E+06 |
| *TM530* | 2.2125 | 2.2023 | 4.6262E+06 | 4.6140E+06 |
| *TM340* | 2.2103 | 2.2021 | 4.6367E+06 | 4.6204E+06 |
| *TM920* | 2.2145 | 2.1996 | 4.4370E+06 | 4.4206E+06 |
| *TM730* | 2.2061 | 2.2012 | 4.2264E+06 | 4.2167E+06 |
| *TM350* | 2.2130 | 2.2028 | 4.2122E+06 | 4.1999E+06 |
| *TM160* | 2.2141 | 2.2094 | 4.1167E+06 | 4.0956E+06 |

thicknesses from 8 to 60 GHz are 0.254mm and 0.508mm, respectively.

### B. THE SELECTION OF THE OPERATION MODES

The high-order mode can provide a high quality factor. However, the higher the high-order modes adopted, the smaller the separation among those high-order modes. That would lead to a narrow band extraction. Hence, at low frequency band, a relative lower-order mode can be chosen for achieving a wideband extraction, for example, the fundamental mode, i.e., $TM_{0,1,0}$, is chosen for a wideband extraction from 8 to 60 GHz. At higher frequency band, since the quality factor of the low-order mode is too small, a high-order mode should be chosen.

The extraction errors of the proposed method are mainly from the fabrication tolerance and the installation error of the measurement, especial for high millimeter-wave frequency extraction. As can be seen from (13)-(18), the effective radius of the CSIW resonator, i.e. $R_{eff}$, plays an important role in the extraction process. As an example, the extracted results at 12.61 GHz from the measured $S_{21}$ of the 0.508 mm thick TLY-5 substrate based PCB are $\varepsilon_r = 2.208$, $\sigma_{eff} = 1.749E + 07\ S/m$ and $\tan\delta = 9.01\text{E} - 04$. When the radius of the CSIW resonator increases by 0.02mm (0.2%), the extracted equivalent dielectric constant rises 0.363% to 2.216, the effective conductivity drops 3.15% to 1.694E + 07 S/m and the dielectric loss tangent reduces 1.62% to 8.864E-04. These errors caused by fabrication tolerance are acceptable. As for the installation error of the measurement, it can be reduced by multiple measurements.

**TABLE 8.** Comparisons between proposed and reported extraction methods.

| Reference | Cavity type | Extraction BW (GHz) | Limitation of $f_H/f_L$ | Cavity number | Excitation form |
|---|---|---|---|---|---|
| [18] | RSIW | 12-19<br>16-26 | <1.58<br><1.63 | 2<br>2 | Microstrip<br>Microstrip |
| [19] | RSIW | 89-105 | <1.18 | 8 | Waveguide |
| [20] | RSIW | 60-110 | <1.83 | 13 | GSG |
| [21] | RSIW | 28-40<br>75-110 | <1.43<br><1.47 | 1<br>1 | Waveguide<br>Waveguide |
| This work | CSIW | 8-60<br>75-110 | ~7.5<br><1.47 | 1<br>1 | GCPW<br>Waveguide |

Table 8 summarizes the comparison between this proposed and reported extraction methods. In order to extract the electrical characteristics of PCB within 8-60 GHz, at least three groups of RSIW resonators are required by the traditional resonator methods. The proposed method overcomes the limitation of frequency bandwidth of RSIW resonators and accurately extracts extremely wideband complex dielectric permittivity and effective conductivity by using one pair of CSIW resonators. In addition, the proposed method has lower costs and less measurement errors.

## V. EXPERIMENTAL VERIFICATIONS

Based on the extracted results of TLY-5Z substrate with thickness of 0.254mm, a fourth order Chebyshev filter is

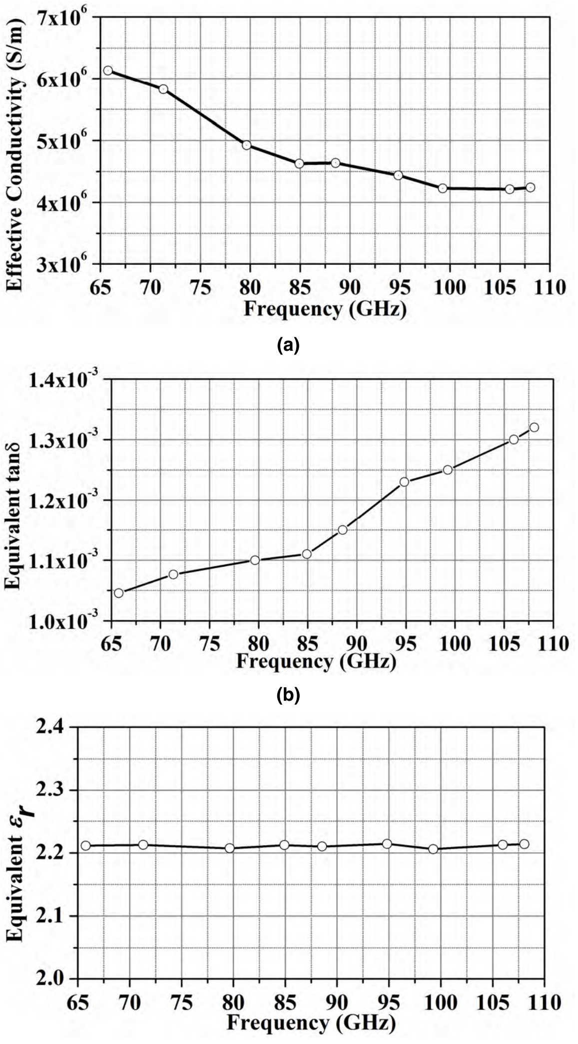

**FIGURE 9.** Extracted equivalent dielectric properties and conductivity of a TYL-5Z PCB within V-band and W-band; (a) Effective conductivity; (b) Dielectric loss tangent; (c) Relative dielectric constant from $h = 0.508$ mm thick substrate.

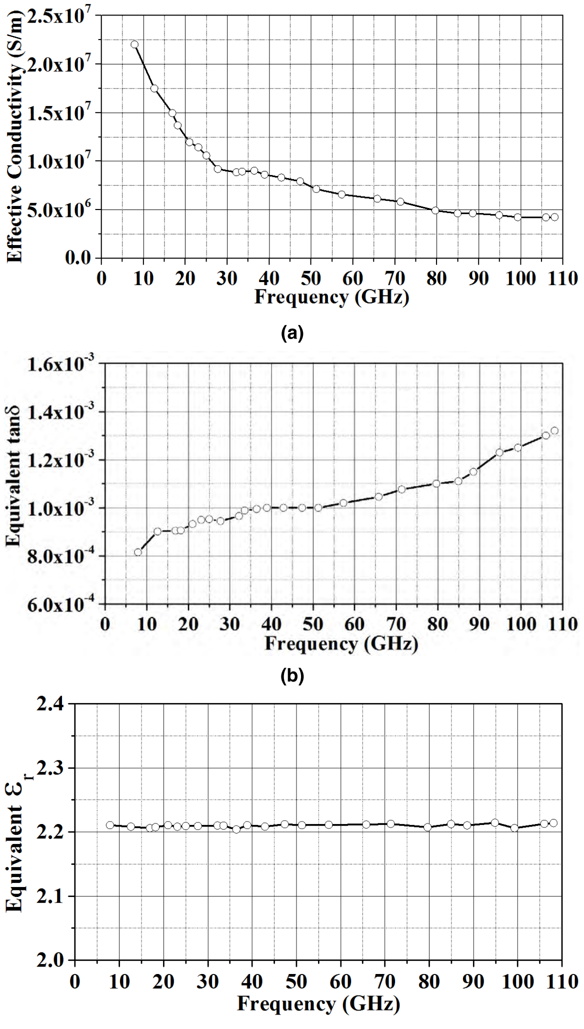

**FIGURE 10.** Measured Printed-Circuit-Board Properties: (a) Effective conductivity; (b) Dielectric loss tangent; (c) Relative dielectric constant from $h = 0.508$ mm thick substrate.

**TABLE 9.** Dimensions of the filters (Unit: mm).

| $W_1$ | $W_2$ | $W_3$ | $W_4$ | $L_1$ | $L_2$ | $L_3$ |
|---|---|---|---|---|---|---|
| 0.76 | 4 | 5.1 | 4.9 | 3 | 11.95 | 12.45 |

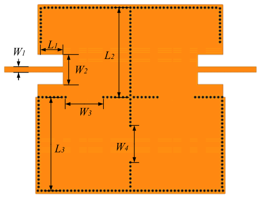

**FIGURE 11.** Configuration of the fourth order Chebyshev filter.

designed at X band. The topological structure is presented in Fig. 11 and the dimensions are listed in table 9. As shown in Fig. 12, the filter is fabricated and measured by using the Keysight Vector Network Analyzer (VNA) and the Anritsu Test Fixture SC5225.

From Fig. 13 (a), compared with the responses of the filter based on the extracted results of TLY-5Z substrate, the responses of the filter designed on the substrate with relative dielectric constant of 2.2 shift 70MHz to the high frequency. In Fig. 13 (b), the measured results of the fourth order Chebyshev filter are in excellent agreement with the simulated results of the filter based on the extracted results. The insertion loss error between the simulation and measurement is around 0.08 dB at 11 GHz. The error is mainly caused by the fabrication tolerance. In addition, the test fixture has a radiation loss, which becomes worse at high frequency band. Therefore, it can be concluded that the extraction of electrical characteristics of PCB guides to accurately design microwave and millimeter-wave filters.

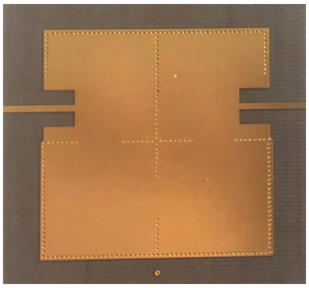

**FIGURE 12.** **Photograph of the fabricated filter.**

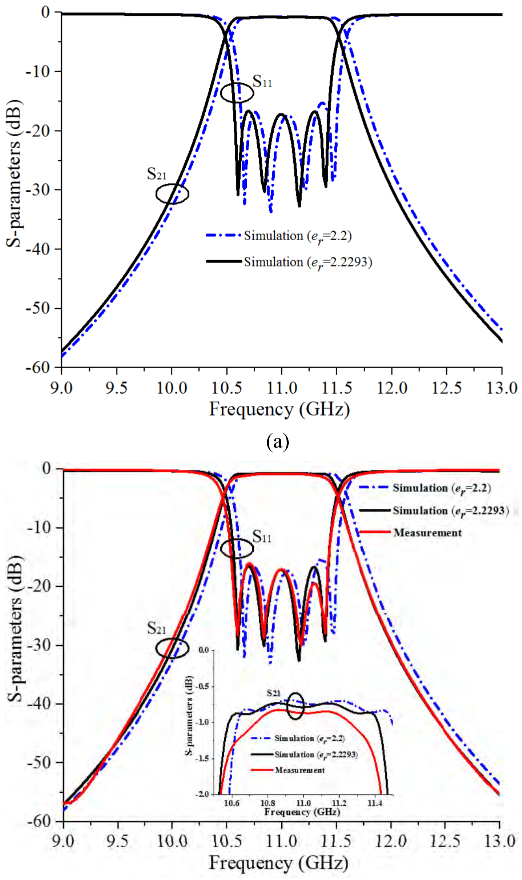

(a)

(b)

**FIGURE 13.** **Simulated and measured S-parameters. (a) Simulation; (b) Measurement.**

## VI. CONCLUSION

In this paper, by utilizing the wideband resonating frequency distribution of multiple high-order $TM_{mn0}$ modes in a CSIW cavity, the equivalent dielectric loss, metal loss, and relative dielectric constant of PCB can be separately extracted over an extremely wide frequency band by only using a small number of CSIW resonators. Comparing with the conventional method, the proposed method has higher efficiency, lower costs and less measurement errors. Experiments, which extract the equivalent dielectric characteristics and conductivity of a TLY-5Z substrate based printed circuit board within 8-110 GHz, have demonstrated the merits of the proposed method. In addition, it should be mentioned, since the proposed method is based on the resonator-extraction method, it would be failed if a very high lossy substrate or a metal needs to be investigated because it is very hard to discriminate the resonating peaks from measured $S_{21}$ results for the extraction due to a very low quality factor for that case.

## REFERENCES

[1] Y. F. Tang, K. Wu, and N. K. Mallat, "Development of substrate-integrated waveguide filters for low-cost high-density RF and microwave circuit integration: Direct-coupled cavity bandpass filters with Chebyshev response," *IEEE Access*, vol. 63, no. 3, pp. 1313–1325, 2015.

[2] M. Kheir, T. Kröger, and M. Höft, "A new class of highly-miniaturized reconfigurable UWB filters for multi-band multi-standard transceiver architectures," *IEEE Access*, vol. 5, pp. 1714–1723, 2017.

[3] Z.-C. Guo *et al.*, "Triple-mode cavity bandpass filter on doublet with controllable transmission zeros," *IEEE Access*, vol. 5, pp. 6969–6977, 2017.

[4] M. Soltani, M. Freyburger, R. Kulkarni, R. Mohr, T. Groezinger, and A. Zimmermann, "Reliability study and thermal performance of LEDs on molded interconnect devices (MID) and PCB," *IEEE Access*, vol. 6, pp. 51669–51679, 2018.

[5] J, Li, J. Shi, L. Li, T. A. Khan, J. Chen, Y. Li, and A. Zhang, "Dual-band annular slot antenna loaded by reactive components for dual-sense circular polarization with flexible frequency ratio," *IEEE Access*, vol. 6, pp. 64063–64070, 2018.

[6] Z. C. Hao, X. Liu, X. Huo, and K. K. Fan, "Planar high-gain circularly polarized element antenna for array applications," *IEEE Trans. Antennas Propag.*, vol. 63, no. 5, pp. 1937–1948, May 2015.

[7] Z.-C. Hao, W.-Q. Ding, and W. Hong, "Developing low-cost *W*-band SIW bandpass filters using the commercially available printed-circuit-board technology," *IEEE Trans. Microw. Theory Techn.*, vol. 64, no. 6, pp. 1775–1786, Jun. 2016.

[8] J. Xu, Z. N. Chen, X. Qing, and W. Hong, "140-GHz planar broadband LTCC SIW slot antenna array," *IEEE Trans. Antennas Propag.*, vol. 60, no. 6, pp. 3025–3028, Jun. 2012.

[9] W. Yang, Y. Yang, W. Che, C. Fan, and Q. Xue, "94-GHz compact 2-D multibeam LTCC antenna based on multifolded SIW beam-forming network," *IEEE Trans. Antennas Propag.*, vol. 65, no. 8, pp. 4328–4333, Aug. 2017.

[10] A. Nafe, F. A. Ghaffar, M. F. Farooqui, and A. Shamim, "A ferrite LTCC-based monolithic SIW phased antenna array," *IEEE Trans. Antennas Propag.*, vol. 65, no. 1, pp. 196–205, Jan. 2017.

[11] Z.-W. Miao *et al.*, "140 GHz high-gain LTCC-integrated transmit-array antenna using a wideband SIW aperture-coupling phase delay structure," *IEEE Trans. Antennas Propag.*, vol. 66, no. 1, pp. 182–190, Jan. 2018.

[12] K. X. Wang, X. F. Liu, Y. C. Li, L. Z. Lin, and X. L. Zhao, "LTCC filtering rat-race coupler based on eight-line spatially-symmetrical coupled structure," *IEEE Access*, vol. 6, pp. 262–269, 2018.

[13] K.-W. Qian, G.-L. Huang, J.-J. Liang, B. Qian, and T. Yuan, "An LTCC interference cancellation device for closely spaced antennas decoupling," *IEEE Access*, vol. 6, pp. 68255–68262, 2018.

[14] L. Zhao, F. Liu, X. Shen, G. Jing, Y.-M. Cai, and Y. Li, "A high-pass antenna interference cancellation chip for mutual coupling reduction of antennas in contiguous frequency bands," *IEEE Access*, vol. 6, pp. 38097–38105, 2018.

[15] F. Fesharaki, C. Akyel, and K. Wu, "Broadband permittivity measurement of dielectric materials using discontinuity in substrate integrated waveguide," *Electron. Lett.*, vol. 49, no. 3, pp. 194–196, Jan. 2013.

[16] X. Wang and A. Stelzer, "Millimeter-wave material characterization using laminated waveguides," *IEEE Trans. Microw. Theory Techn.*, vol. 62, no. 8, pp. 1762–1771, Aug. 2014.

[17] C. A. Jones, "Permittivity and permeability measurements using stripline resonator cavities-a comparison," *IEEE Trans. Instrum. Meas.*, vol. 48, no. 4, pp. 843–848, Aug. 1999.

[18] X.-C. Zhu *et al.*, "Extraction of dielectric and rough conductor loss of printed circuit board using differential method at microwave frequencies," *IEEE Trans. Microw. Theory Techn.*, vol. 63, no. 2, pp. 494–503, Feb. 2015.

[19] Y. J. Cheng and X. L. Liu, "W-band characterizations of printed circuit board based on substrate integrated waveguide multi-resonator method," *IEEE Trans. Microw. Theory Techn.*, vol. 64, no. 2, pp. 599–606, Feb. 2016.

[20] D. E. Zelenchuk, V. Fusco, G. Goussetis, A. Mendez, and D. Linton, "Millimeter-wave printed circuit board characterization using substrate integrated waveguide resonators," *IEEE Trans. Microw. Theory Techn.*, vol. 60, no. 10, pp. 3300–3308, Oct. 2012.

[21] H. B. Wang and Y. J. Cheng, "Broadband printed-circuit-board characterization using multimode substrate-integrated-waveguide resonator," *IEEE Trans. Microw. Theory Techn.*, vol. 65, no. 6, pp. 2145–2152, Jun. 2017.

[22] S. C. Chen *et al.*, "A dielectric constant measurement system for liquid based on SIW resonator," *IEEE Access*, vol. 6, pp. 41163–41172, 2018.

[23] D.-Y. Kim, W.-S. Chung, C.-H. Park, S.-J. Lee, and S. Nam, "A series slot array antenna for 45°-inclined linear polarization with SIW technology," *IEEE Trans. Antennas Propag.*, vol. 60, no. 4, pp. 1785–1795, Apr. 2012.

[24] J. Wu, Y. J. Cheng, and Y. Fan, "60-GHz substrate integrated waveguide fed cavity-backed aperture-coupled microstrip patch antenna arrays," *IEEE Trans. Antennas Propag.*, vol. 63, no. 3, pp. 1075–1085, Mar. 2015.

[25] Q.-L. Yang, Y.-L. Ban, K. Kang, C.-Y.-D. Sim, and G. Wu, "SIW multibeam array for 5G mobile devices," *IEEE Access*, vol. 4, pp. 2788–2796, 2016.

[26] Q.-L. Yang, Y.-L. Ban, J.-W. Lian, Z.-F. Yu, and B. Wu, "SIW butler matrix with modified hybrid coupler for slot antenna array," *IEEE Access*, vol. 4, pp. 9561–9569, 2016.

[27] M. S. Abdallah, Y. Wang, W. M. Abdel-Wahab, and S. S. Naeini, "Design and optimization of SIW center-fed series rectangular dielectric resonator antenna array with 45° linear polarization," *IEEE Trans. Antennas Propag.*, vol. 66, no. 1, pp. 23–31, Jan. 2018.

[28] Z. Gan, Z. Tu, and Z. Xie, "Pattern-reconfigurable unidirectional dipole antenna array fed by SIW coupler for millimeter wave application," *IEEE Access*, vol. 6, pp. 22401–22407, 2018.

[29] X. Li, J. Xiao, Z. Qi, and H. Zhu, "Broadband and high-gain SIW-fed antenna array for 5G applications," *IEEE Access*, vol. 6, pp. 56282–56289, 2018.

[30] J.-X. Zhuang, Z.-C. Hao, and W. Hong, "Silicon micromachined terahertz bandpass filter with elliptic cavities," *IEEE Trans. THz Sci. Technol.*, vol. 5, no. 6, pp. 1040–1047, Nov. 2015.

[31] Y.-W. Wu, Z.-C. Hao, M.-C. Tao, and W. Hong, "Extracting extremely wideband complex dielectric permittivity and effective conductivity by using one pair of SIW circular cavities," in *Proc. IEEE MTT-S Int. Wireless Symp. (IWS)*, May 2018, pp. 1–3.

[32] J. Gu, Y. Fan, and Y. Zhang, "A low-loss SICC filter using LTCC technology, for X-Band application," in *Proc. Int. Conf. Appl. Superconductivity Electromagn. Devices (ASEMD)*, Sep. 2009, pp. 152–154.

[33] J. M. Fu, "Microwave resonator," in *Advanced Electromagnetic Theory*, vol. 7, 1st ed. Xi'an, China: Xi'an Jiaotong Univ. Press, 2000, pp. 201–202.

[34] *DataSheet for the TLY-5Z Substrate*. Accessed: Jul. 10, 2018. [Online]. Available: http://www.4taconic.com/uploads/ADD%20Data%20Sheets/1510763061_Taconic%20TLY-5Z%20Technical%20Data%20Sheet.pdf

[35] *Ansiru Test Fixture Wensite*. Accessed: Jul. 10, 2018. [Online]. Available: https://www.anritsu.com/zh-cn/components-accessories/products/3680-series

**YI-WEN WU** (S'18) received the B.S. degree in electronics and information engineering from Xidian University, Xi'an, China, in 2016. He is currently pursuing the Ph.D. degree in electromagnetic field and microwave technology with Southeast University, Nanjing, China.

His current research interests include the design of passive filters and antennas at millimeter-wave, and terahertz frequency band.

**ZHANG-CHENG HAO** (M'08–SM'15) received the B.S. degree in microwave engineering from Xidian University, Xi'an, China, in 1997, and the M.S. and Ph.D. degrees in radio engineering from Southeast University, Nanjing, China, in 2002 and 2006, respectively.

In 2006, he joined the Laboratory of Electronics and Systems for Telecommunications, École Nationale Supérieure des Télécommunications de Bretagne, Bretagne, France, as a Postdoctoral Researcher, where he was involved in developing millimeter-wave antennas. In 2007, he joined the Department of Electrical, Electronic and Computer Engineering, Heriot-Watt University, Edinburgh, U.K., as a Research Associate, where he was involved in developing multilayer integrated circuits and ultra-wide-band components. In 2011, he joined the School of Information Science and Engineering, Southeast University, Nanjing, as a Professor. He has authored or coauthored over 180 referred journal and conference papers. He holds 20 granted patents. His current research interests include microwave and millimeter-wave systems, submillimeter-wave and terahertz components and passive circuits, including filters, antenna arrays, couplers, and multiplexers. He was a recipient of the Thousands of Young Talents presented by China Government, in 2011, and the High Level Innovative and Entrepreneurial Talent presented by Jiangsu Province, China, in 2012. He is an Associate Editor of the *IET Microwaves Antennas & Propagation* and *Electronics Letters* and a Guest Editor of the IEEE T-MTT Special Issue on IWS 2018. He has served as a Reviewer for many technique journals, including the IEEE Transactions on Microwave Theory and Techniques, the IEEE Transactions on Antennas and Propagation, IEEE AWPL, and IEEE MWCL.

**MING-CUI TAO** received the B.S. degree in electronics and information engineering from Xidian University, Xi'an, China, in 2016. She is currently pursuing the M.S. degree in electromagnetic field and microwave technology with Southeast University, Nanjing, China.

Her current research interests include microwave and millimeter passive components, and antennas.

**XIANG WANG** (S'18) was born in Nanjing, Jiangsu, China. He received the B.S. degree in electrical engineering from the Nanjing University of Science and Technology, Nanjing, in 2014. He is currently pursuing the Ph.D. degree in electromagnetic field and microwave technology with Southeast University, Nanjing.

His current research interests include miniaturized passive circuits, oscillators, and millimeter-wave transceiver systems.

Mr. Wang is a Reviewer for four international journals, including *Electronics Letters*, the *International Journal of RF and Microwave Computer-Aided Engineering*, *Microwave and Optical Technology Letters*, and *IET Microwaves, Antennas and Propagation*.

**JIA-SHENG HONG** received the D.Phil. degree in engineering science from the University of Oxford, Oxford, U.K., in 1994.

His doctoral dissertation was on electromagnetic (EM) theory and applications. In 1994, he joined the University of Birmingham, where he focused on microwave applications of high-temperature superconductors, EM modeling, and circuit optimization. In 2001, he joined the Department of Electrical, Electronic and Computer Engineering, Heriot-Watt University, Edinburgh, U.K., as a Faculty Member, where he leads a team for research into advanced RF/microwave device technologies. He has authored or coauthored over 130 journal and conference papers. He has also authored *Microstrip Filters for RF/Microwave Applications* (Wiley, 2001) and *RF and Microwave Coupled-Line Circuits*, Second Edition (Artech House, 2007). His current research interests include RF/microwave devices, such as antennas and filters, for wireless communications and radar systems, as well as novel material and device technologies including RF microelectromechanical systems (MEMS), and ferroelectric and high-temperature superconducting devices.